Available online at www.sciencedirect.com
ScienceDirect
Advances in Space Research 45 (2010) 1235–1243
ADVANCES IN SPACE RESEARCH (a COSPAR publication)
www.elsevier.com/locate/asr

Investigation of vertical profile of rain microstructure at Ahmedabad in Indian tropical region

Saurabh Das [a], Ashish K. Shukla [b], Animesh Maitra [a,*]

[a] Institute of Radio Physics and Electronics, University of Calcutta, Kolkata 700 009, India
[b] Space Applications Centre, Indian Space Research Organization, Ahmedabad 380 015, India

Received 24 June 2009; received in revised form 31 December 2009; accepted 5 January 2010

Abstract

The microstructure of rain has been studied with observations using a vertical looking Micro Rain Radar (MRR) at Ahmedabad (23.06°N, 72.62°E), a tropical location in the Indian region. The rain height, derived from the bright band signature of melting layer of radar reflectivity profile, is found to be variable between the heights 4600 m and 5200 m. The change in the nature of rain, classified on the basis of radar reflectivity, is also observed through the MRR. It has been found that there are three types of rain, namely, convective, mixed and stratiform rain, prevailing with different vertical rain microstructures, such as, Drop Size Distribution (DSD), mean drop size, rain rate, liquid water content and average fall speed of the drops at different heights. It is observed that the vertical DSD profile is more inhomogeneous for mixed and stratiform type rain than for convective type rain. It is also found that the large number of drops of size <0.5 mm is present in convective rain whereas in stratiform rain, drops concentration is appreciable up to 1 mm. A comparison of measurements taken by ground based Disdrometer and that from the 200 m level obtained from MRR shows good agreement for rain rate and DSD at smaller rain rate values. The results may be useful for understanding rain structures over this region.

Keywords: Bright band; Rain microstructure; Rain drop size distribution; Tropical rainfall; Micro Rain Radar

1. Introduction

Rain is the most dominant impairment for the propagation of millimeter waves. Rain attenuation models are based on the properties of rain drops and interaction between rain drops and electromagnetic waves (Crane, 1996). The Drop Size Distribution (DSD) is an important parameter for calculation of rain attenuation. Rain attenuation is found to be different for different rain types of same rain intensity due to the characteristics change of rain DSD (Maitra and Chakravarty, 2005). It also depends on the vertical extent of rain up to rain height. The ITU-R model (2005a,b) is based on the simplified assumption of constant rain height derived from the zero degree isotherm height and a uniform vertical rain structure (Ajayi and Barbalis-cia, 1990). These assumptions may not be valid for tropical regions and lead to unsatisfactory results.

It is well known that the rain characteristics are largely different in tropics from the temperate counterparts (Green, 2004). ITU-R recommendations are based on extensive study in temperate regions. The vertical structure of rain thus can give useful insight in the process peculiar to the tropical region. Vertical profiles of rain for different temperate regions have been reported using Doppler radar, Micro Rain Radar (MRR), etc. by different researchers (Clemens et al., 2006; Peters et al., 2006; Peter et al., 2002). But, there is a dearth of observations in the tropical region, especially for India (Kunhikrishnan et al., 2006; Cha et al., 2007). It is thus required to identify the actual vertical rain structure and test the assumptions for different rain types for this region.

Indian Space Research Organization (ISRO) is currently planning to conduct a "Ka Band Propagation Experiment"

* Corresponding author. Tel.: +91 33 2350 9116; fax: +91 33 2351 5828.
E-mail addresses: animesh.maitra@gmail.com, am.rpe@caluniv.ac.in (A. Maitra).

0273-1177/$36.00 © 2010 COSPAR. Published by Elsevier Ltd. All rights reserved.
doi:10.1016/j.asr.2010.01.001

to estimate the rain attenuation at Ka band over India. For this purpose, a Ka band beacon transmitter will be sent with GSAT-4 satellite. Different instruments like Micro Rain Radar (MRR), Disdrometer and Raingauge are deployed at different locations over India to measure different meteorological parameters associated with rain. For the present study, vertical profile of rain has been observed with a vertically pointing MRR at Ahmedabad (23.06°N, 72.62°E). A Disdrometer is also used to measure the drop size at the ground level.

In this paper, we present some preliminary results based on a few case studies during monsoon periods of the year 2006. The possibility of rain classification using MRR is investigated and used in this study.

Vertical profiles of rain microstructures, such as, mean drop size, rain rate, liquid water content and average fall speed of the drops have been analysed here for different rain types from propagation point of view. This will provide better understanding and insight into the physical processes of rain attenuation. The DSD characteristics of MRR are also compared with that of ground based Disdrometer. The current study is an attempt to demonstrate the usefulness of such analysis for rain attenuation study in the tropical region.

2. Experimental setup and data collection

2.1. Data collection

At Ahmedabad (23.06°N, 72.62°E), located in the western part of India, rain mainly occurs in the monsoon period (i.e. July–September). The vertical profiles of rain parameters are observed using a MRR. It has a temporal resolution of 30 s and vertical resolution of 200 m. The 200 m resolution is taken to accommodate the nearly complete profile of the rain up to 6 km over the Indian region. A Disdrometer, located adjacent to MRR, is used to collect DSD information at ground level. It also has an integration time of 30 s.

The Disdrometer and MRR are located 150 m apart in an open ground and can be said to be exposed to the same rain conditions. The instruments are operated based on different physical principle, thus providing independent measurement of the same rain event. MRR measures the backscattered signal from the rain drops to calculate different microphysical parameters at different heights whereas Disdrometer measures the momentum of the rain drops at ground. Thus Disdrometer depends on mechanical principle whereas MRR depends on electromagnetic interaction. Details of the instruments are provided in the following subsection.

2.2. Description of the Instruments

2.2.1. MRR

MRR is an FM-CW Doppler radar which operates at 24.1 GHz. It provides DSD information by converting measured Doppler spectra into drop diameters by known relationship. Various microphysical parameters can thus be reliably estimated without any assumption to the DSD shape.

The DSD is calculated for drop diameters from 0.245 to 4.53 mm with falling velocities from 0.78 to 8.97 m/s. The retrieval of Doppler spectra, DSD and different microphysical parameters are described by Strauch (1976) and Peter et al. (2002). Rain rate (R), liquid water content (LWC), and radar reflectivity (Z) are calculated from the DSD. Mean fall velocity is calculated directly from the measured Doppler spectrum.

The spectral volume reflectivity $\eta(f)$ received by the radar from range gate centered at r with the depth δr is given by,

$$\eta(r,f)\,df = p(r,f)\,df \cdot C \cdot \frac{r^2}{\delta r} t^{-1}(r) \tag{1}$$

where $p(r,f)$ is spectral power, f is Doppler frequency in Hz and C is radar constant.

The DSD is calculated from the volume reflectivity $\eta(D)$ related to the spectral reflectivity $\eta(f)$ and single particle scattering cross-section (D) as follows:

$$n(D) = \frac{\eta(D)}{\sigma(D)} \tag{2}$$

where (D) is calculated using Mie theory.

Using the following formulae, the integral parameters from the DSD have been estimated (Peter et al., 2002):

$$\mathrm{LWC} = \frac{\pi}{6}\rho_w \int_0^\infty D^3 n(D)\,dD \tag{3}$$

$$R = \frac{\pi}{6}\int_0^\infty D^3 v(D) n(D)\,dD \tag{4}$$

$$Z = \int_0^\infty n(D) D^6\,dD \tag{5}$$

$$D_m = \int_0^\infty \frac{D n(D)\,dD}{n(D)\,dD} \tag{6}$$

where LWC is the liquid water content in mg/m^3, R is the rain rate in mm/h, Z is the radar reflectivity in dB, D_m is the mean drop diameter in mm, ρ_w is the density of water, D is the diameter of the drops in mm. $n(D)$ is the number of drops with the size D to $D + \Delta D$ in mm^{-1} m^{-3}, $v(D)$ is the fall velocity of drops with the size D to $D + \Delta D$ in m/s.

Mean fall velocity is obtained as fallows:

$$v_m = \frac{\lambda}{2}\frac{\int_0^\infty f \cdot p(f)\,df}{\int_0^\infty p(f)\,df} \tag{7}$$

where v_m is the mean fall velocity in m/s, λ is the Wavelength. $p(f)$ is the spectral power related to Doppler frequency.

Corrections for lower air densities leading to higher falling velocities in high altitudes are applied. Errors due to non-spherical drops are within 6% at 10 mm/h and neglected for this study.

2.2.2. Disdrometer

The Disdrometer, RD-80, is a Joss type drop size counter and has the ability to transform the vertical momentum of the drops to an electrical signal whose amplitude is a function of the drop diameter. Using the Gunn and Kinzer (1949) relation, drop diameter is estimated from the terminal velocity. It provides drop size information in 20 bins in range of 0.3–5.5 mm. From the actual measurements of DSD, rain rate (R) in mm/h has been obtained as follows:

$$R = \frac{\pi}{6}\frac{3.6}{10^3}\frac{1}{A\cdot t}\sum_{i=1}^{20}\left(n_i D_i^3\right) \tag{8}$$

where A is the total area of observation, t is the integration time, n_i is the number of drops for size class i. D_i is the mean diameter of size class i.

It is assumed that the momentum is entirely due to the terminal fall velocity of the drops and drops are spherical. Errors due to acoustic noises are minimized by installing the instrument at the roof top of a building. The Disdrometer becomes insensitive for a time period after a bigger drop strikes and called 'dead time'. This 'dead time' leads to underestimation of the smaller drops that fall within this period. But, the effects of these smaller drops are less on rain attenuation and are within 5% error limit (Tokay and Short, 1996). For this study dead time correction has not been applied.

3. Rain classification scheme

Classification of rain is an important research topic in radar meteorology. It is very useful for a large number of applications, from improvement of radar estimation of rainfall in remote sensing to rain attenuation estimation at higher frequencies. There are various methodology developed to discriminate the rain type. Houze (1993) proposed use of vertical air velocity and hydrometeor fall velocity for classification of rain since vertical air motion is small compared to the fall velocity of hydrometeor in stratiform rain (Rao et al., 2001). Rain rate threshold criteria are also used for rain classification (Johnson and Hamilton, 1988). Gamache and Houze (1982) also proposed using radar reflectivity factor of 38 dBz as a threshold value for such purpose. Waldvogel (1974), based on his observation of N_0 jump of the exponential drop size distribution, proposed rain classification based on drop size distribution. Similar methodology of using drop size distribution is also reported by Tokay and Short (1996).

Here we used the method for rain classification which is based on the vertical radar reflectivity profile. The stratiform rain type can be identified by the "bright band" signature in radar reflectivity profile. The bright band is the enhanced back scattered part of vertical radar reflectivity profile due to the presence of melting layer. The melting layer has larger reflectivity than the water droplet. It appears like a bright region in the radar reflectivity profile as if heavy rain is occurring at that height. The existence of melting layer is a definite signature of stratiform type of rain (Fabry and Zawadzki, 1995). The reason behind this is the fact that melting layer can only form when there is no strong up-drift, which is only satisfied in stratiform rain condition. This method has been utilized with MRR data using time series of vertical radar reflectivity profile up to 6 km to classify the rain (Kunhikrishnan et al, 2006; Cha et al. 2007) and also with TRMM measurements (Awaka et al., 1998). The maximum reflectivity in the instantaneous profile gives the height of the bright band. The maximum positive and negative gradient gives the lower and upper limit of the melting layer (Klaassen, 1988).

The convective type of rain is characterized by the absence of any bright band. A transition state or mixed state may occur between these two distinct phases. This state can be identified by two prominent peaks in radar reflectivity due to presence of melting layer and liquid rain at two distinct heights. This type of rain can occur for a good percentage of time in a year (Rao et al., 2001).

The automated bright band identification is a critical process. The presence of false peak can wrongly be identified as bright band. Similarly, the initial phase of bright band formation can easily be overlooked due to a small enhancement of reflectivity profile. These may leads to improper classification of rain. The error can be minimized by imposing simultaneous criteria instead of simply taking the maximum peak reflectivity. Since the bright band occurs due to melting layer, thus it should only appear near the 0 °C isotherm height. It is also to be noted that taking continuous measurement also reduces the possibility of misidentification of bright band as any random peak will be removed in larger set. However, once bright band associated with melting layer is identified properly, the rain can be classified as stratiform type.

4. Experimental observations

The time series of vertical reflectivity of MRR is studied for different rain events. Once the bright band is observed in the profile, a more in depth study in terms of different rain parameters is performed. The drop size distribution observed by MRR at 200 m level is then compared with the measurement taken by Disdrometer, providing a better understanding of the results as well as validity of MRR measurement.

The MRR data of the monsoon of 2006 reveal quite a number of events with the prominent bright band. A few examples of such events are shown in Fig. 1(a)–(c) for different dates and time span mentioned in the figure.

Here, we present an analysis of the typical rain event observed on 15 August 2006 occurring from 16:21:30 UTC to 20:43:30 UTC. Maximum rain for the observed period is about 10.02 mm/h at ground. The total observation time is 4 h 22 min. The radar reflectivity (Z) for the observed period has been depicted in Fig. 1(a) which shows the evolution of bright band during the rain event between 4.6 km and 5.2 km.

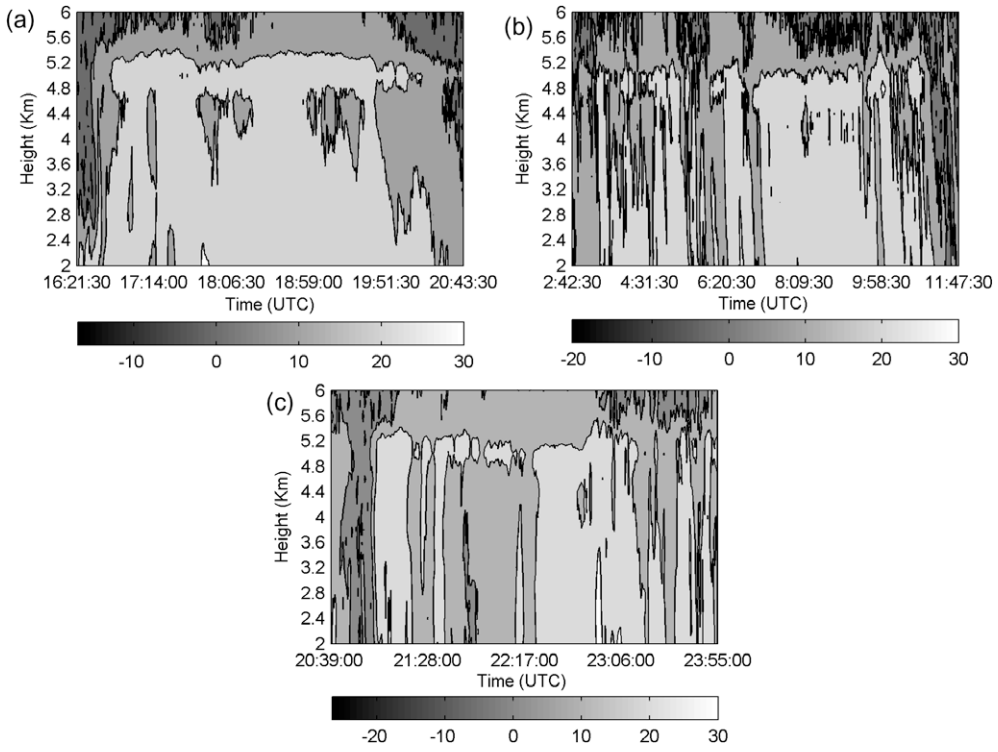

Fig. 1. Radar reflectivity profile for: (a) 16:21:30–20:43:30 UTC of 15/08/2006; (b) 02:42:30–11:47:30 UTC of 01/08/2006; and (c) 20:39:30-23:55:00 UTC of 03/07/2006.

Further, investigations of the time evolution of the rain event of 15 August 2006 help to classify rain types at different time instants. It is found that around 16:42:30 UTC no bright band is visible, at around 17:10:30 UTC bright bands with two peaks and at around 17:33:30 UTC, a clear bright band structure is visible. These are representative of convective, mixed and stratiform rain type, respectively.

Continuous measurements of radar reflectivity profiles for these three cases are shown in Fig. 2(a)–(c). This also reduces the uncertainty in the measurement up to some extent. In Fig. 2(a), radar reflectivity factor monotonically decreases with height, indicating absence of bright band whereas Fig. 2(c) clearly shows the existence of bright band indicated by large enhancement of reflectivity around 5 km. The enhanced reflectivity around 3 km and 5 km are also prominent in Fig. 2(b), indicating a mixed nature of rain.

Detailed descriptions of the characteristics of these rain types at that time spans are given in the following subsections including radar reflectivity, rain rate, liquid water content, mean drop size distribution and average fall velocity.

4.1. Rain with no bright band

The vertical profiles of different rain parameters, as obtained from MRR, are shown in Fig. 3 for the rain event on 15th August, 2006. In Fig. 3(a), radar reflectivity profile is given for 16:40:00 UTC to 16:44:30 UTC, which shows that no bright band is present, indicating that the rain type is convective (Kunhikrishnan et al, 2006; Williams et al, 1995). The convective rain is associated with vertical wind motion prohibiting formation of melting layer. Different integral rainfall parameters are shown in Figs. 3(b)–(f). The profile of rain rate in Fig. 3(b) shows a small enlargement near 3.0 km with a peak in LWC as shown in Fig. 3(c), but a decrease in the average fall velocity is indicated in Fig. 3(d) and a decrease in mean drop diameter in Fig. 3(e). The weighted mean drop diameter decreases with increasing height with occasional increase in diameter. The overall vertical variation of diameter is found to be increasing with height. Drop concentrations at different heights are shown in Fig. 3(f) for measurement at 16:42:30 UTC. From Fig. 3(f), it can be seen that the drop concentrations are more at smaller diameters region, although maximum drop diameter reaches nearly up to 3.4 mm at 200 m height.

4.2. Rain with two peaks

At time from 17:08:30 UTC to 17:13:30 UTC on the same day, the vertical profiles of different parameters are shown in Fig. 4. The vertical profile of radar reflectivity in Fig. 4(a) shows two peaks near 3.0 km and near 5.0 km. The peak near 5.0 km can be assumed to be the actual bright band. The reason is that the bright band occurs near the zero degree isotherm which in case of Ahmedabad is around 5.0 km. The enhancement of reflectivity around 5.0 km is thus contributed to the presence of the melting layer.

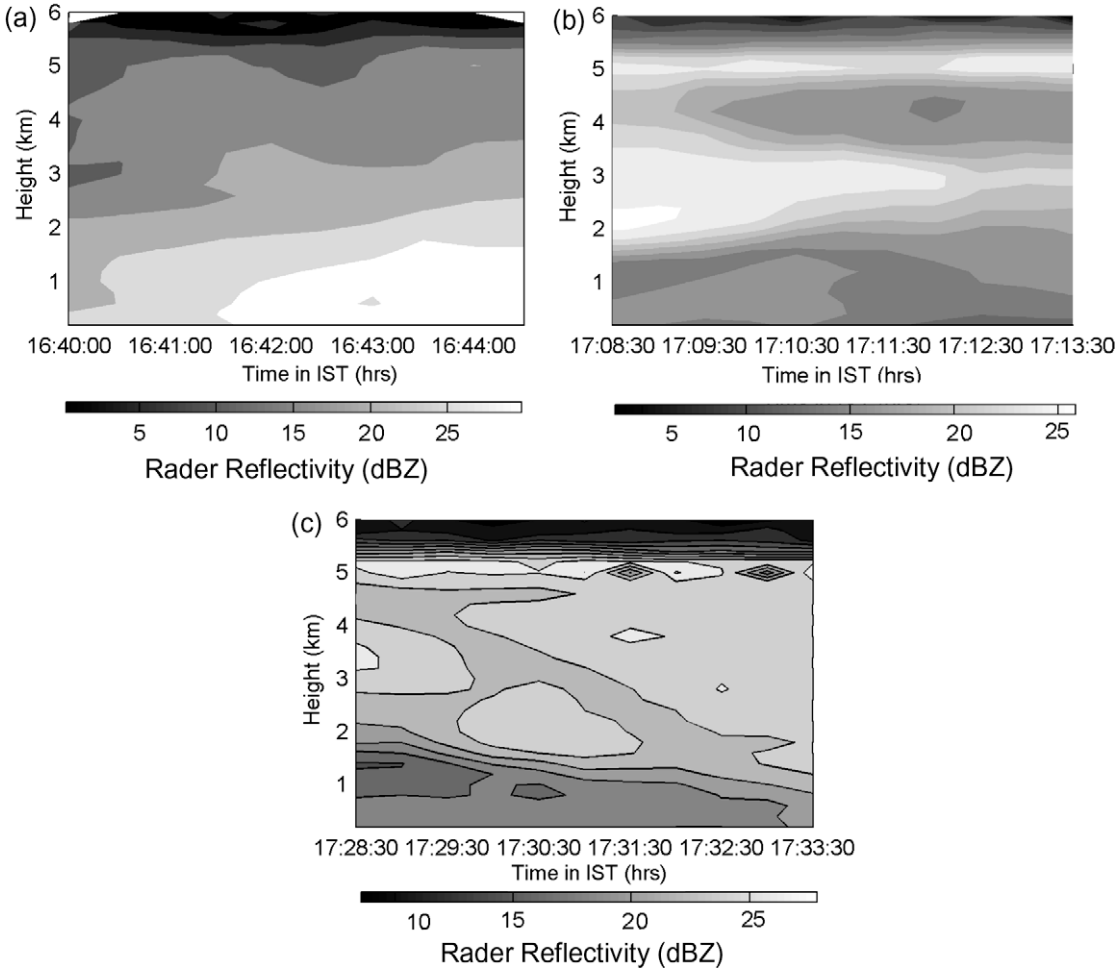

Fig. 2. Radar reflectivity profile of 15/08/2006 for: (a) 16:40:00–16:44:30 UTC; (b) 17:08:30–17:13:30 UTC; and (c) 17:28:30–17:33:30 UTC.

A smaller but broader peak is also visible around 3.0 km which may be caused by the liquid rain. This indicates that the formation of bright band occur around 5.0 km level with embedded small scale convective activity. The maximum intensity corresponding to the liquid rain occurs at lower height may be due to this convection process. The average fall velocity also shows a broader peak at this level (Fig. 4(d)). This event corresponds to a mixture of the convective type with stratiform type rain (Steiner et al., 1995; Awaka et al., 1998).

Rain rate and LWC profiles are shown in Fig. 4(b) and (c). They show almost uniform structure with height. The weighted mean drop diameter is characterized by almost similar drop size as shown in Fig. 4(e). The vertical variation of drop size distribution at 17:10:30 UTC is shown in Fig. 4(f). The drop breakup process seems dominating below 2 km and coalescence is dominating process above 2–4 km, as shown from the vertical profile of DSD given in Fig. 4(f). The apparent bigger drops at 5 km are due to the presence of melting layer and not realistic. The maximum drop size reaches up to 1.5 mm near the ground.

4.3. Rain with clear bright band

The vertical profiles as given by MRR from 17:28:30 UTC to 17:33:30 UTC on 15 August are shown in Fig. 5. The vertical radar reflectivity shows a clear peak at 5.0 km that corresponds to the melting layer as shown in Fig. 5(a). This type of rain is clearly identified as a stratiform rain. However, an increase in reflectivity does not indicate an increase in rain rate around 5.0 km in Fig. 5(b) as the enhanced peak is not due to liquid rain but due to the melting layer. LWC also has a clear peak at this level as shown in Fig. 5(c). Whereas for the profile of fall velocity as shown in Fig. 5(d), the peak appears before 5.0 km. Similar observations were reported by Peter et al. (2002) and Kunhikrishnan et al. (2006).

The mean drop diameter approximately decreases with increase in height up to 3 km. The sharp peak around 5 km is an artifact and seems to be due to the presence of melting layer. A significant variation is seen in the over all profile.

The vertical DSD at 17:30:30 UTC is shown in Fig. 5(f). The drops with drop diameters up to 2 mm are found at

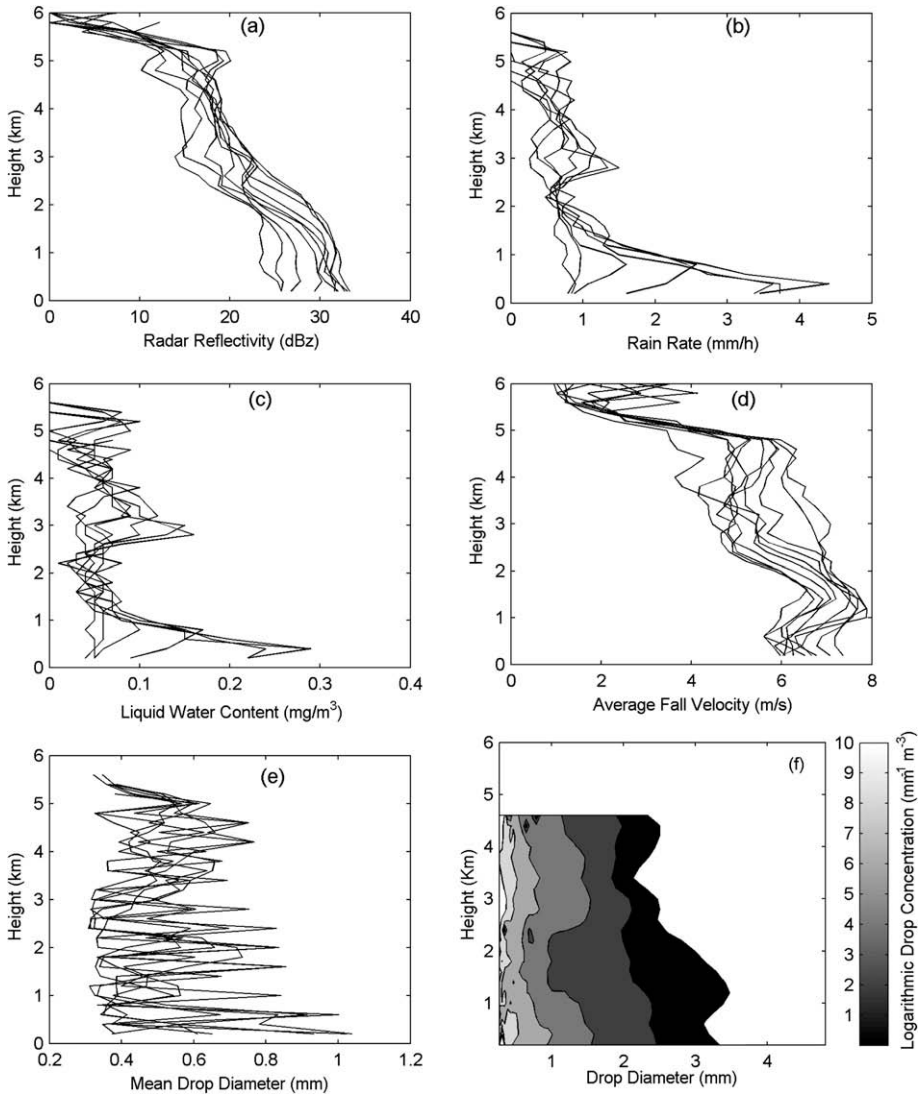

Fig. 3. vertical profiles of different rain parameters obtained by MRR at 16:40:00–16:44:30 UTC of 15th August 2006: (a) radar reflectivity profile, (b) rain rate, (c) liquid water content, (d) average fall velocity, (e) mean drop diameter, and (f) drop size distribution at 16:42:30 UTC.

200 m level, although more bigger drops are abundant at higher levels. The vertical profile of DSD shows drop breakup process dominates throughout the entire height range.

4.4. Comparison of MRR and Disdrometer observation

The Disdrometer operating at the same place is considered for comparison with MRR observations. The Disdrometer provides drop size information in 20 bins in range of 0.3–5.5 mm whereas the MRR estimates the drop concentration in 42 bins in range of 0.245–5.03 mm. The different measuring principles of the instruments are also helpful to validate the measurements qualitatively. Since the lowest height available from MRR is at 200 m, measurement from this level is compared with the ground based Disdrometer. This will also provide a clue about the extent of applicability of ground measurements for predicting the rain attenuation over an earth-space path.

The actual rain rate measurement both by Disdrometer and MRR show a good agreement as shown in Fig. 6(a). Fig. 6(b) shows the correlation plot of MRR and Disdrometer rain rate measurements and the 1:1 relationship line. Correlation coefficient between two measurements is found to be about 0.8. Scattering of rain rate is higher above 2.5 mm/h. This may be due to the different measuring principle of the instruments and because of the fact that back scattered signal is noisy at high rain rates.

The drop size distribution as observed by the MRR at 200 m and Disdrometer at the ground level are presented in Fig. 7(a)–(c) for three different types of rain. They show different drop size distributions for these three types of rain. Stratiform type is dominated by the bigger drop size both in ground and near-ground measurement as shown in Fig. 7(c), whereas it is the reversed for convective rain, as indicated in Fig. 7(a). Drop size up to 0.5 mm is dominating for convective case, but for stratiform case appreciable numbers of drops are of size up to 1 mm. However, the

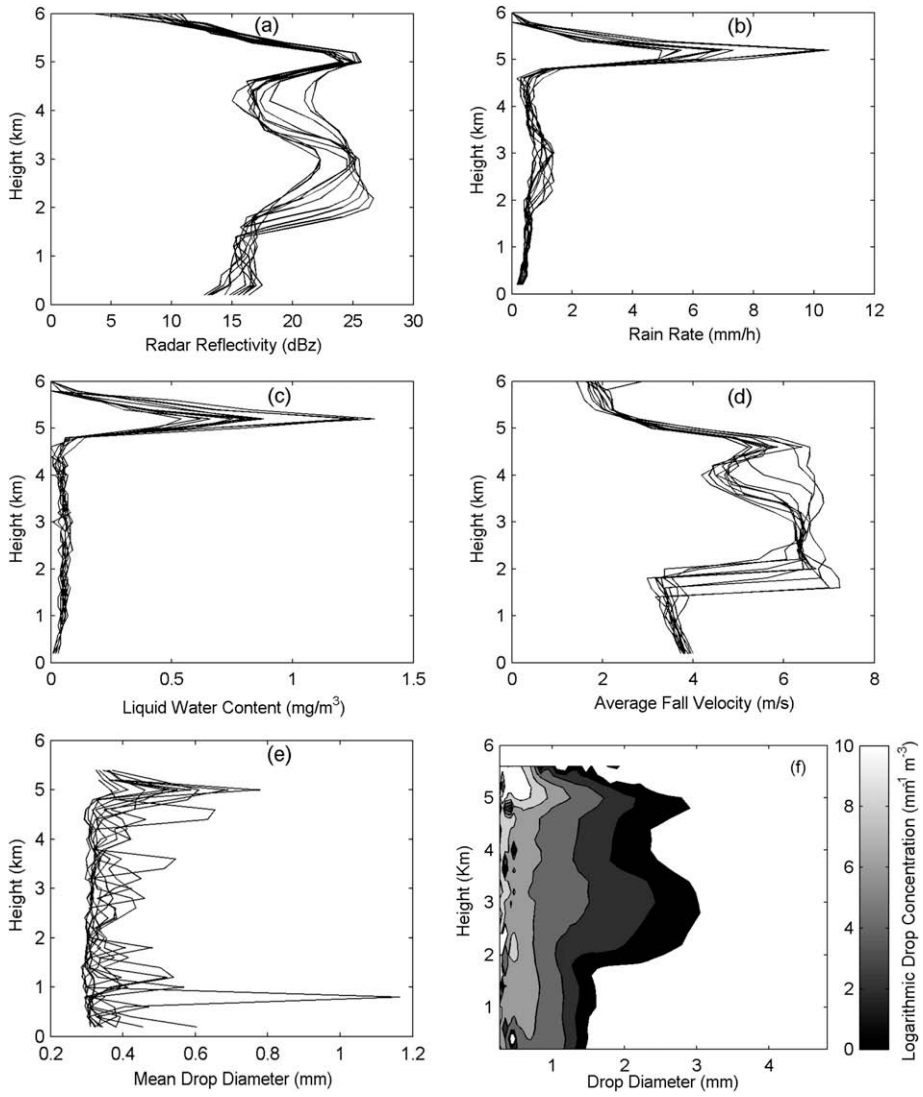

Fig. 4. Vertical profiles of different rain parameters obtained by MRR at 17:08:30–17:13:30 UTC of 15th August 2006: (a) radar reflectivity profile, (b) rain rate, (c) liquid water content, (d) average fall velocity, (e) mean drop diameter, and (f) drop size distribution at 17:10:30 UTC.

reverse features for stratiform and convective rain is also reported (Rao et al., 2001). Mixed state shows an intermediate nature between the two cases (Fig. 7(b)).

In Fig. 7(a), the MRR observations show very high concentrations of smaller drops (~0.3 mm) than the Disdrometer observations. In the convective rain, turbulence may have caused vary small drops to fail to reach the ground level in large numbers. Thus for very small drops of (<0.3 mm) are not prominent in Disdrometer measurements. Also Disdrometer measures drops in the range of 0.3–5.5 mm whereas MRR measures the drops in the range of 0.245–5.03 mm. Thus MRR is more sensitive to the smaller drops than the Disdrometer. For this reasons, the scale mismatch between Disdrometer and MRR is significant only at lower end of the drop size spectrum and comparable otherwise.

5. Discussions and conclusions

Information on rain microstructures of different types of rain is of practical importance for satellite communications at frequencies above 10 GHz. Using a MRR and a ground based Disdrometer observations some case studies of tropical rain over Ahmedabad are presented. From the MRR observation, rain is classified into three different types. These three types of rain are characterized by different microphysical parameters like DSD, fall velocity, LWC, rain rate and radar reflectivity. The observation shows that the nature of rain changes with time during a rain event.

The bright band due to the melting layer is obtained at around 5.0 km but is found to be variable. The co-existence of a prominent peak of reflectivity with the bright band is attributed to the existence of a mixed state. The vertical

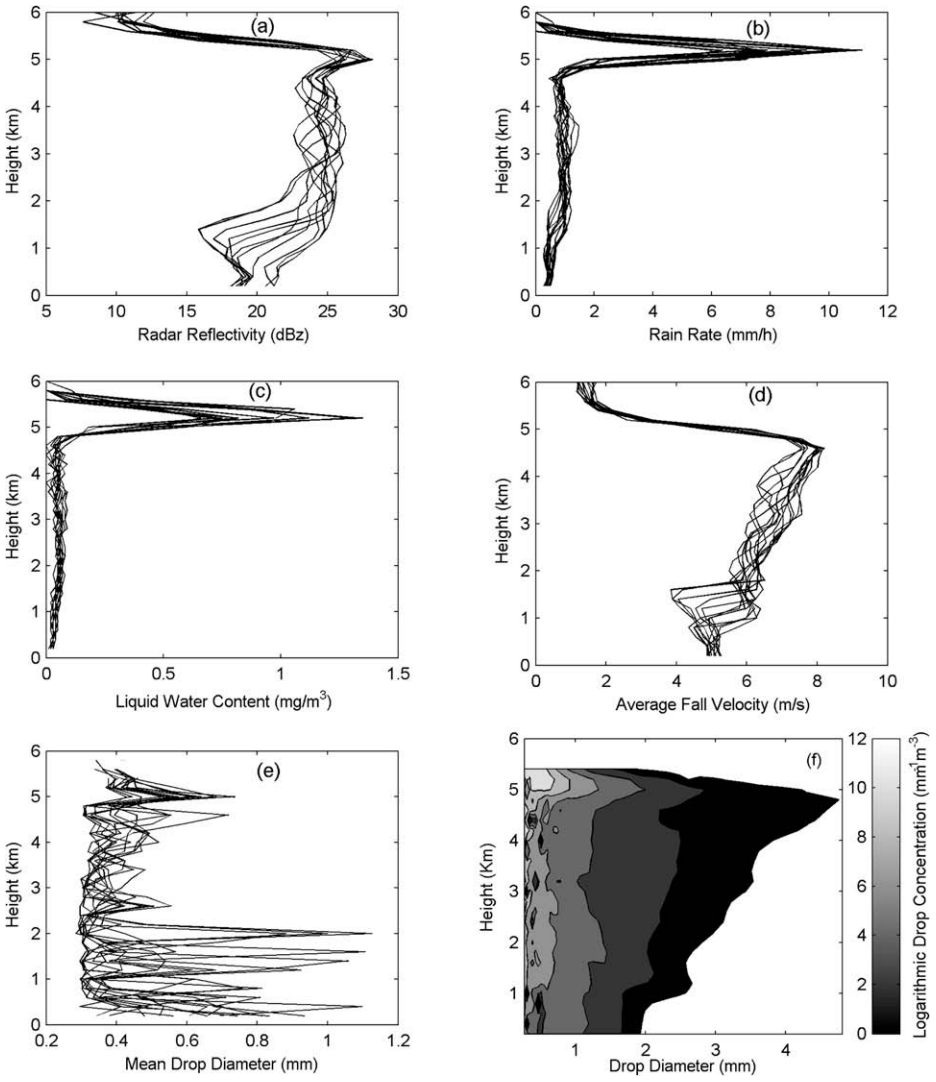

Fig. 5. Vertical profiles of different rain parameters obtained by MRR at 17:28:30–17:33:30 UTC of 15th August 2006: (a) radar reflectivity profile, (b) rain rate, (c) liquid water content, (d) average fall velocity, (e) mean drop diameter, and (f) drop size distribution at 17:30:30 UTC.

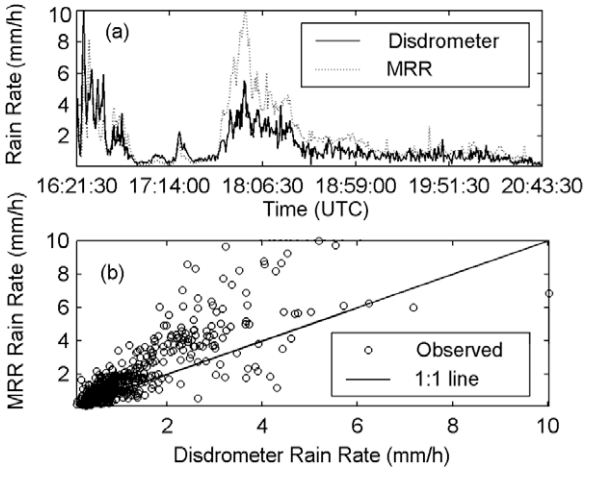

Fig. 6. (a) Comparison of rain rate and (b) the 1:1 relation plot of MRR and Disdrometer measurements of the event observed on 15th August 2006.

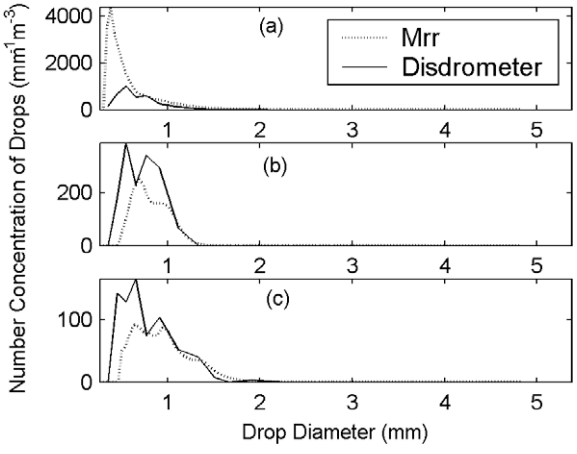

Fig. 7. Comparison of rain DSD for: (a) convective type (16:42:30 UTC), (b) mixed type (17:10:30 UTC), and (c) stratiform type (17:33:30 UTC).

structure of DSD is found to be non-uniform for such mixed and stratiform state which needs further investigations.

The comparison of rain rates with Disdrometer and MRR observation at 200 m shows good agreement and the drop size distribution at different height gives an insight of the physical process associated with rain. It is found from the measurements of DSD at the ground and near-ground levels that the large number of drops of size <0.5 mm is present in convective rain whereas in stratiform rain, drops concentration is appreciable up to 1 mm. However, the maximum drop size of convective rain can be up to 3.4 mm whereas it is only up to 1.8 mm for stratiform rain for the presented sequence of events. The mixed type is an in-between case of convective and stratiform types.

The study highlights the different rain characteristics of tropical location of Ahmedabad. The applicability of the data largely depends on the local climatology. These analyses provide a further insight into the tropical rain structure and are useful for satellite communication links designing at high frequencies for tropical sites.

Acknowledgements

Authors are grateful to scientists of Space Applications Centre, ISRO to assist in maintaining the instrument and data collection. Authors are also sincerely thankful to Mr. Deval Mehta and Dr. K.S. Dasgupta, senior scientists, ISRO, for reviewing the work.

References

Ajayi, G.O., Barbaliscia, F. Prediction of attenuation due to rain: characteristics of the 0 °C isotherm in temperate and tropical climates. Int. J. Satell. Commun. 8, 187–196, 1990.

Awaka, J, Iguchi, T., Okomoto, K. Early results on rain type classification by the tropical rainfall measuring mission (TRMM) precipitation radar, in: Proceedings of the Eighth URSI Commission F Open Symposium, Aveiro, Portugal, pp. 143–146, 1998.

Cha, Joo-Wan, Seong, Soo Yum, Chang, Ki-Ho, Sung, Nam Oh Estimation of the melting layer from a Micro Rain Radar (MRR) data at the Cloud Physics Observation System (CPOS) site at Daegwallyeong Weather Station. APJAS 43 (1), 77–85, 2007.

Clemens Marco, Peters, G., Seltmann, J., Winkler, P. Time–height evolution of measured raindrop size distributions, in: Proceedings of the ERAD, 2006.

Crane, R.K. Electromagnetic Wave Propagation through Rain. University of Oklahoma, 1996.

Fabry, F., Zawadzki, I. Long-term radar observations of the melting layer of precipitation and their interpretation. J. Atmos. Sci. 52, 838–851, 1995.

Gamache, J.F., Houze, R.A. Mesoscale air motions associated with a tropical squall line. Mon. Weather Rev. 110, 118–135, 1982.

Green, H.E. Propagation impairment on Ka-band SATCOM links in tropical and equatorial regions. IEEE Antennas Propag. Mag. 46 (2), 31–45, 2004.

Gunn, R., Kinzer, G.D. The terminal velocity of fall for water droplets in stagnant air. J. Meteorol. 8, 249–253, 1949.

Houze, R.A. Cloud Dynamics. Academic Press, San Diego, CA, 573pp, 1993.

International Telecommunication Union Recommendation P 838-3. Specific attenuation model for rain for use in prediction methods, Propagation in non-ionized media, 2005a.

International Telecommunication Union Recommendation P 893-3. Rain height model for prediction methods, Propagation in non-ionized media, 2005b.

Johnson, R.h., Hamilton, P.J. The relationship of surface features to the precipitation and air flow structure of an intense midlatitude squall line. Mon. Weather Rev. 116, 1444–1472, 1988.

Klaassen, W. Radar observations and simulations of the melting layer of precipitation. J. Atmos. Sci. 45, 3741–3753, 1988.

Kunhikrishnan, P.K., Sivaraman, B.R., Kiran Kumar, N.V.P., Alappattu Denny, P. Rain observations with Micro Rain Radar (MRR) over Thumba, in: Proceedings of the SPIE, 6408 (64080L-1), 2006.

Maitra, A., Chakravarty, K. Raindrop size distribution measurements and associated rain parameters at a tropical location in the Indian region. URSI GA, 2005.

Peter, G., Fischer, B., Anderson, T. Rain observation with a vertically looking Micro Rain Radar (MRR). Boreal Environ. Res. 7, 353–362, 2002.

Peters, G., Fischer, B., Clemens, M. Areal homogeneity of Z–R-relations, in: Proceedings of the ERAD, 2006.

Rao, T.N., Rao, D.N., Mohan, K., Raghavan, S. Classification of tropical precipitating systems and associated Z–R relationships. J. Geophys. Res. 106 (D16), 17699–17711, 2001.

Steiner, M., Houze Jr., R.A., Yuter, S.E. Climatological characterization of three-dimensional storm structure from operational radar and rain gauge data. J. Appl. Meteorol. 34, 1978–2007, 1995.

Strauch, R.G. Theory and applications of FM-CW Doppler radar, Ph.D. Thesis, University of Colorado, 97pp, 1976.

Tokay, A., Short, D. Evidence from tropical rain drop spectra of the origin of rain from stratiform versus convective. J. Appl. Meteorol. 35, 355–371, 1996.

Waldvogel, A. The N_0 jump of raindrop spectra. J. Atmos. Sci. 31, 1067–1078, 1974.

Williams, C.R., Ecklund, W.L., Gage, K.S. Classification of precipitating clouds in the Tropics using 915-MHz wind profiler. J. Atmos. Ocean. Technol. 12, 996–1012, 1995.